Effect of CeO_2 Doping on Phase Structure of AlCoCuFeMnNi High Entropy Alloys

Zhi-xin Wang[1], Ming-xing Ma[1,], Jia-chen Zhou[1], Cun Liang[1], Cong Zhao[2]*

[1]School of Materials and Chemical Engineering, Zhongyuan University of Technology, Zhengzhou, 450007, China

[2]School of Chemistry and Environmental Technology, Chongqing University of Arts and Sciences, Chongqing 402160, China

**E-mail:manager92@163.com*

Abstract: AlCoCuFeMnNi high-entropy alloy was fabricated by non-consumable arc remelter. AlCoCuFeMnNi and AlCoCuFeMnNi + 1wt% CeO_2 alloys were investigated by XRD prepared on their phase structure. The results show that AlCoCuFeMnNi alloy has BCC1+BCC2 dual phase structure. 1wt% CeO_2 addition improves the diffraction peak of AlCoCuFeMnNi alloy. **T**he mixing entropy is 13.38J ·mol-1 ·K-1, the mixing enthalpy is -2.56kJ ·mol-1, the atomic radius difference is 0.15, and the Gibbs free energy is -35.73kJ ·mol-1 for AlCoCuFeMnNi high-entropy alloy.

Keywords: High-entropy alloy; AlCoCuFeMnNi; Phase structure; Microstructure

1. INTRODUCTION

The design concepts of the high entropy alloys (HEAs) have more than five main alloying elements and each element having 5at% - 35at%, which is markedly different from the design idea of traditional alloy [1-13]. The existing research results show that HEAs have simple phase (such as FCC, BCC, FCC+BCC， FCC+FCC and BCC+BCC) and many excellent properties[2-13]. Zhang[2] reported that FeCrNiCoMnBx high-entropy alloy coating was prepared by laser cladding on a low carbon steel substrate, and the coating had a simple FCC structure with boride precipitation. Boride precipitation was mainly the (Cr,Fe)2B phase when the boron content x was increased from 0.25 to 0.75. Choudhuri[3] reported that the phase structure of AlxCuCrFeNi2 changed the primary solidification phase from a simple disordered-FCC to a bcc-based ordered-B2 phase with increment of Al content from x=0.8 to x=1.0 (+6at%), and a second solidification product forms, a disordered-BCC in case of x = 0.8 and a disordered-fcc in case of x = 1.0. Li[4] reported that HEA fibers with diameters ranging from 1 to 3.15 mm in diameter, with the composition of $Al_{0.3}$CoCrFeNi (atomic percent, at.%), were successfully fabricated by hot-drawing, and these analyses revealed a homogeneous FCC structure in the as-cast material, while post processing produced nanosized B2 particles in an FCC matrix. Shang[5] reported that the final milling products for as-milled CoCrFeNi($W_{1-x}Mo_x$) (x = 0, 0.5) coating powders are the mixture of BCC and FCC solid solution phases, while order FCC phase exists for CoCrFeNiW. VHPS-ed CoCrFeNiW and CoCrFeNi$W_{0.5}Mo_{0.5}$ HEACs are 600 and 650μm in thickness respectively, and bear a good metallurgical bonding to the substrate. Both HEACs comprise two FCC phases with a small amount of δ-NiW and σ-CoCr phases. Mohanty[6] reported that MA powder showed the presence of FCC (τ) and BCC (κ) solid solution phases, indicated that BCC (κ) solid solution undergoes eutectoid transformation during sintering leading to the formation of L12 ordered α′ and σ phases, whereas FCC (τ) phase remains unaltered with a slight change in the lattice parameter. Tan[7] reported that CoCrFeNiMnPd eutectic high-entropy alloy was designed and prepared, and through a series of experimental characterization and theoretical analysis, it could be concluded that the sluggish diffusion effect of high-entropy alloys makes the interface deviate considerably from the local non-equilibrium condition and the alternate arrangement of CoCrFeNiPd-rich FCC and Tetragonal Mn_7Pd_9 lamellae results in weak interface energy anisotropy, thus forming the seaweed eutectic-dendrite. Li[11] reported that the pressure– volume relationship of the AlCoCrCuFeNi high-entropy alloy at room temperature had been studied using in situ high-pressure energy-dispersive x-ray diffraction with synchrotron radiation at high pressures. The equation of state of the AlCoCrCuFeNi HEA was determined by the calculation of the radial distribution function. The experimental results indicate that the HEA keeps a stable FCC+BCC structure in the experimental pressure range from 0 GPa to 24 GPa. In this paper, AlCoCuFeMnNi high entropy alloy was prepared by melting casting method. The influence of CeO2 doping on its phase structure were discussed in detail, providing theoretical guidance for the theoretical system improvement and subsequent research of high

entropy alloy.

2. EXPERIMENTAL

AlCoCuFeMnNi high-entropy alloy was fabricated by noon-consumable arc remelter. The pure metals of Al, Co, Cu, Fe, Ni and Mn with 200 mesh size and higher purity than 99.5wt% were used as raw materials. The above metal powders having equal molar ratio were mixed by ball milling, compacted, and prepared using WK type non-consumable arc melting furnace under argon environment. The alloy ingot was smelted five times in order to obtain unifrom composition. The preparation process of CeO_2 doping sample was identical to that of the samples without doping. The cast ingot was cut into 10mm*10mm*5mm block samples by DK7716 electrical discharge machining(EDM). The crystal structure and phase purity of the synthesized samples were identified by x-ray diffraction (XRD) analysis using an Rigaku Ultima IV X-ray diffractometer with Cu Kα radiation operated at 40kV and 30mA. Diffraction data were recorded range from 30 °to 80 °.

3. RESULTS AND DISCUSSION

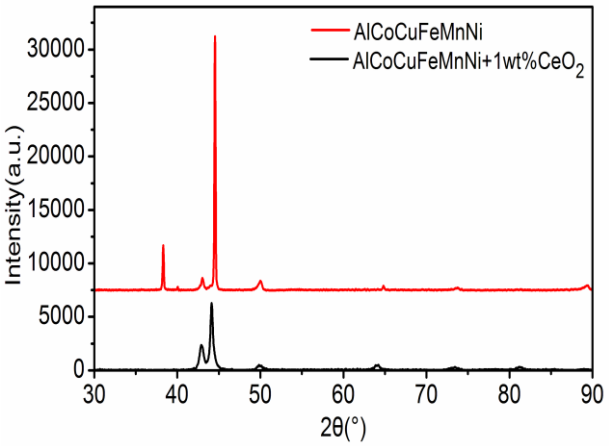

Figure 1. XRD patterns of AlCoCuFeMnNi and AlCoCuFeMnNi + 1wt CeO_2 high-entropy alloy

Figure 1 is the XRD patterns of the AlCoCuFeMnNi alloy and AlCoCuFeMnNi + 1wt CeO_2 alloy. As can be seen from Figure 1, the two alloys are double BCC phase. After doping 1wt% CeO_2, the intensity of diffraction peaks had a significant improvement. This was because the rare earth elements can improve the decontamination of alloy solution, the performance and the grain refinement of cast alloys. Thus, the crystallinity of the alloy was enhanced and the diffraction peaks enhanced [9]. Owing to high mixing entropy effect, the phase structures of the two alloys had no intermetallic compounds. Compared with the lattice extinction rule, the phase structure was composed by two kinds of BCC phases for AlCoCuFeMnNi high-entropy alloy. The diffraction peaks of BCC1 were belonged to (111), (200), (220) and (311) crystal planes. The diffraction peaks of BCC2 were corresponded to (111), (200), (220), (311) and (222) crystal planes. According to the Gibbs free energy law [14-16]:

$$\Delta G_{mix} = \Delta H_{mix} - T\Delta S_{mix} \quad (1)$$

Where ΔH_{mix} is the mixing enthalpy, T is the thermodynamic temperature, and ΔS_{mix} is the mixed entropy. From the Eq. 8, the mixing enthalpy and the mixed entropy were two competition factors for the change of the system free energy. There was beneficial to the reduce of system free energy, alloy ordering and segregation trend with the increment of the mixed entropy especially at high temperature, which made the disordered solid solution formed easily compared with the intermetallic compounds during solidification. Based on the Boltzmanna hypothesis of the relationship between entropy and system confusion, the alloy mixed entropy ΔS_{mix} can be expressed as [16]:

$$\Delta S_{\text{mix}} = -R\sum_{i=1}^{n} c_i \ln c_i \quad (2)$$

$$\Delta S_{\text{mix}} = R\ln n \quad (3)$$

Table1 Mixed enthalpy between the various elements[17] (kJ/mol)

	Al	Co	Cu	Fe	Mn	Ni	Ce
Al	–	-19	-1	-11	-19	-22	-38
Co	-19	–	6	-1	-5	0	-18
Cu	-1	6	–	13	4	4	-21
Fe	-11	−1	13	–	0	-2	3
Mn	−19	-5	4	0	–	-8	1
Ni	-22	0	4	-2	-8	–	-28
Ce	-38	-18	-21	3	1	-28	

Where ci is the mole percent of the i-th component in the alloy system ($\sum_{i=1}^{n} c_i = 1$), and R is the gas constant. The mixing enthalpy ΔH_{mix} can be expressed as [4,16]:

$$\Delta H_{mix} = \sum_{i=1, i\neq j}^{n} \Omega_{ij} c_i c_j \quad (4)$$

$$\Omega_{ij} = 4\Delta H_{AB}^{mix} \quad (5)$$

Where Ωij is the interaction parameter of component between the i-th and the j-th elements, ΔH_{AB}^{mix} is the enthalpy of mixing for the binary equal atomic A-B alloy calculated by the Miedema model[17]. Table1 was the mixed enthalpy between the various elements[17]. According to the Hume-Ruthery rule, the

atomic radius difference δ can be expressed as:

$$\delta=\sqrt{\sum_{i=1}^{n} c_i\left(1-\frac{r_i}{\bar{r}}\right)^2} \quad (6)$$

$$\bar{r}=\sum_{i=1}^{n} c_i r_i \quad (7)$$

Where r_i is the atomic radius of i component, is the average atomic radius of the alloy components[18-22]. Table2 was element characteristic parameters of AlCoCuFeMnNi and AlCoCuFeMnNi + 1wt CeO_2 alloy. From Eq. 1-7, the mixing entropy is 13.38J mol-1 K-1, the mixing enthalpy is -2.56kJ mol-1, the atomic radius difference is 0.15, and the Gibbs free energy is -35.73kJ mol-1 for AlCoCuFeMnNi high-entropy alloy. The mixing entropy is 13.54J mol-1 K-1, the mixing enthalpy is -2.78kJ mol-1, the atomic radius difference is 0.56, and the Gibbs free energy is -37.73kJ mol-1 for AlCoCuFeMnNi + 1wt CeO_2 high-entropy alloy.

Table2 Element characteristic parameters of AlCoCuFeMnNi and AlCoCuFeMnNi + 1wt CeO_2 alloy

Element	Melting point (℃)	Electronegativity	Atomic radius (nm)	Lattice structure
Al	660	1.61	0.143	FCC
Co	1495	1.88	0.125	HCP/BCC
Cu	1083	1.90	0.128	FCC
Fe	1535	1.83	0.127	BCC/FCC
Mn	1244	1.55	0.126	BCC
Ni	1453	1.92	0.125	FCC
Ce	798	1.12	0.182	FCC

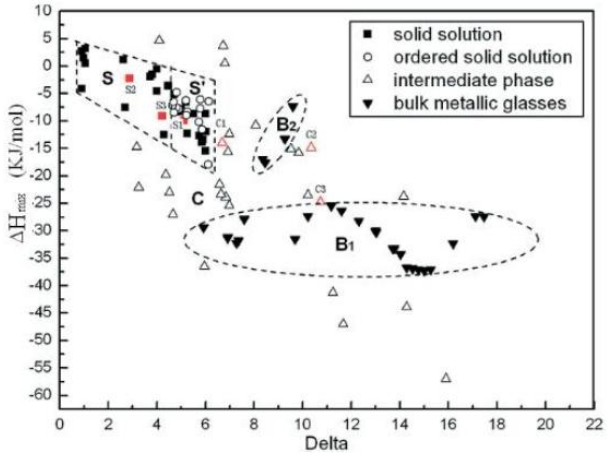

Figure 2. Relationship between delta and ΔH_{mix} for MHAs and typical multicomponent bulk metallic glasses[21]

Figure 2 was relationship between delta and ΔH_{mix} for MHAs and typical multicomponent bulk metallic glasses[21]. For comparison, the corresponding parameters of the typical multicomponent bulk metallic glasses were also calculated. According to the above calculation results, AlCoCuFeMnNi and AlCoCuFeMnNi + 1wt CeO_2 high-entropy alloy were belonged to the area of solid solution.

4. CONCLUSIONS

AlCoCuFeMnNi and AlCoCuFeMnNi + 1wt CeO2 alloy had double BCC phase. After doping 1wt% CeO2, the intensity of diffraction peaks had a significant improvement becasue rare earth elements can improve the decontamination of alloy solution, the performance and the grain refinement of cast alloys. The diffraction peaks of BCC1 were belonged to (111), (200), (220) and (311) crystal planes. The diffraction peaks of BCC2 were corresponded to (111), (200), (220), (311) and (222) crystal planes. The mixing entropy is 13.38J mol-1 K-1, the mixing enthalpy is -2.56kJ mol-1, the atomic radius difference is 0.15, and the Gibbs free energy is -35.73kJ mol-1 for AlCoCuFeMnNi high-entropy alloy. The mixing entropy is 13.54J mol-1 K-1, the mixing enthalpy is -2.78kJ mol-1, the atomic radius difference is 0.56, and the Gibbs free energy is -37.73kJ mol-1 for AlCoCuFeMnNi + 1wt CeO2 high-entropy alloy. According to the above calculation results, AlCoCuFeMnNi and AlCoCuFeMnNi + 1wt CeO2 high-entropy alloy were belonged to the area of solid solution.

ACKNOWLEDGMENT

This work was supported by the Scientific and Technological Project of Chongqing, China (Grant No. CSTC, 2009AB4171), and the Innovation Foundation for Technology Based Firms of Ministry of Science and technology, China (Grant No. 04C26225100807).

REFERENCES

[1] J. W. Yeh, S. K. Chen, S. J. Lin, J. Y. Gan, T. S. Chin, T. T. Shun, C. H. Tsau, and S. Y. Chang, Nanostructured high-entropy alloys with multiple principal elements: novel alloy design concepts and outcomes. Adv. Eng. Mater. 2004,6: 299-303.

[2] C. Zhang, B. Wu, Q. Wang, D. Chen, and P. Dai, Microstructure and Properties of FeCrNiCoMnBx High-Entropy Alloy Coating Prepared by Laser Cladding, Rare Metal Mat. Eng., 2017,9:1230-1234.

[3] D. Choudhuri, B. Gwalani, S. Gorsse, C. V. Mikler, R. V. Ramanujan, M. A. Gibson, and R. Banerjee, Change in the primary solidification phase from fcc to bcc-based B2 in high entropy or complex concentrated alloys, Scripta Mater., 2017, 127: 186-190.

[4] D. Li, C. Li, T. Feng, Y. Zhang, G. Sha, J. J. Lewandowski, P. K. Liaw, and Y. Zhang, High-entropy Al0.3CoCrFeNi alloy fibers with high tensile strength and ductility at ambient and cryogenic temperatures, Acta Mater., 2017, 123: 285-294.

[5] C. Shang, E. Axinte, J. Sun, X. Li, P. Li, J. Du, P. Qiao, and Y. Wang, CoCrFeNi($W_{1-x}Mo_x$) high-entropy alloy coatings with excellent mechanical properties and corrosion resistance prepared by mechanical alloying and hot-pressing sintering, Mater. Des., 2017, 117:193-202.
[6] S. Mohanty, T. N. Maity, S. Mukhopadhyay, S. Sarkar, N. P. Gurao, S. Bhowmick, and K. Biswas, Powder metallurgical processing of equiatomic AlCoCrFeNi high entropy alloy: Microstructure and mechanical properties, Mater. Sci. Eng.: A, 2017, 679: 299-313
[7] Y. Tan, J. Li, J. Wang, and H. Kou, Seaweed eutectic-dendritic solidification pattern in a CoCrFeNiMnPd eutectic high entropy alloy, Intermetallics, 2017, 85:74-79.
[8] M.X. Ma, D.C. Zhu, M.J. Tu. The effect of Eu^{2+} doping concentration on luminescence properties of $BaAl_2Si_2O_8:Eu^{2+}$ blue phosphor, Acta Phys. Sin. -Ch. Ed. 58 (2009) :5826-5830
[9] M. X. Ma, D. C. Zhu, C. Zhao, et al. Effect of Sr^{2+}-doping on structure and luminescence properties of $BaAl_2Si_2O_8:Eu^{2+}$ phosphors, Opt. Commu. 285(2012):665-668.
[10] G.H. Meng, X. Lin, H. Xie, et al, The effect of Cu rejection in laser forming of AlCoCrCuFeNi/Mg composite coating, Mater. Des. 108(2016): 157-167
[11] G. Li, D.H. Xiao, P.F. Yu, et al, Equation of state of an AlCoCrCuFeNi high-entropy alloy, JOM, 67(2015):2310-2313
[12] Y. Deng, C.C. Tasan, K.G. Pradeep, et al, Design of a twinning-induced plasticity high entropy alloy, Acta Mater. 94(2015):124-133
[13] M.J. Yao, K.G. Pradeep, C.C. Tasan, et al, A novel, single phase, non-equiatomic FeMnNiCoCr high-entropy alloy with exceptional phase stability and tensile ductility, Scripta Mater. s72-73 (2014) :5-8
[14] R.S. Ganji, P.S. Karthik, K.B.S. Rao, et al, strengthening mechanisms in equiatomic ultrafine grained AlCoCrCuFeNi high-entropy alloy studied by micro- and nanoindentation methods, Acta Mater. 125(2017):58-68
[15] Y.J. Zhou, Y. Zhang, Y.L. Wang, et al, Solid solution alloys of AlCoCrFeNiTix with excellent room-temperature mechanical properties, Appl. Phys. Lett. 90 (2007):181904
[16] T.M. Yue, H. Xie, X. Lin, et al. Solidification behaviour in laser cladding of AlCoCrCuFeNi high-entropy alloy on magnesium substrates, J. Alloys Compd. 587(2014):588-593
[17] A. Takeuchi, A. Inoue, Classification of bulk metallic glasses by atomic size difference, heat of mixing and period of constituent elements and its application to characterization of the main alloying element, Mater. Trans. 46(2005): 2817-2829.
[18] J. M. Zhu, H.F. Zhang, H.M. Fu, et al. Microstructures and compressive properties of multicomponent AlCoCrCuFeNiMox alloys, J. Alloys Compd. 497(2010):52-56
[19] L.H. Wen, H.C. Kou, J.S. Li, et al. Effect of aging temperature on microstructure and properties of AlCoCrCuFeNi high-entropy alloy, Intermetallics, 17(2009):266-269
[20] Y. Zhang, X. Yang, P.K. Liaw, Alloy design and properties optimization of high-entropy alloys, JOM, 64 (2012) :830-838
[21] Y. Zhang, Y. Zhou, J. Lin, et al, Solid-solution phase formation rules for multi-component alloys, Adv. Eng. Mater. 10(2010) :534-538
[22] Q.Y. Zhai, C. Jia, Z.X. Kang, et al. Microstructure and capacitor discharge\par welding characteristics of quenched Cu25Al10Ni25Fe20Co20 high-entropy alloy foils, Acta Metall. Sin. 47 (2011) :1378-1381